Song, S., Cai, S., Han, D., García Nuñez, C., Zhang, G., Wallace, G., Fleming, L., Craig, K., Reid, S., Martin, I. W., Rowan, S., & Gibson, D. (2023). Tantalum oxide and silicon oxide mixture coatings deposited using microwave plasma assisted co-sputtering for optical mirror coatings in gravitational wave detectors. *Applied Optics*, *62*(7), B73-B78. https://doi.org/10.1364/ao.477211

Tantalum Oxide and Silicon Oxide Mixture Coatings Deposited Using Microwave Plasma Assisted Co-sputtering for Optical Mirror Coatings in Gravitational Wave Detectors

SHIGENG SONG[1,4,*], SIJIA CAI[1], DAXING HAN[1], CARLOS GARCÍA NUÑEZ[1], GONG ZHAN[5], GAVIN WALLACE[2], LEWIS FLEMING[1], KIERAN CRAIG[2], STUART REID[2], IAIN MARTIN[3], SHEILA ROWAN[3], DES GIBSON[1,4]

[1]*Institute of Thin Films, Sensors and Imaging, University of the West of Scotland, SUPA, Paisley PA1 2BE, Scotland, UK*
[2]*University of Strathclyde, SUPA Glasgow G1 1XQ, Scotland, UK*
[3]*University of Glasgow, SUPA Glasgow G12 8QQ, Scotland, UK*
[4]*Albasense, Scotland, UK*
[5]*Optoelectronic Engineering, Changchun University of Science and Technology, China*

[1]*Des.Gibson@uws.ac.uk*
**Shigeng.Song@uws.ac.uk*

Received XX Month XXXX; revised XX Month, XXXX; accepted XX Month XXXX; posted XX Month XXXX (Doc. ID XXXXX); published XX Month XXXX

Abstract: This work presents the characterization of optical and mechanical properties of thin films based on $(Ta_2O_5)_{1-x}(SiO_2)_x$ mixed oxides deposited by microwave plasma assisted co-sputtering, including post annealing treatments. Deposition of low mechanical loss materials (3×10^{-5}) with high refractive index (1.93) while maintaining low processing costs was achieved and the following trends were demonstrated: energy band gap increases as SiO2 concentration increases in the mixture and disorder constant decreases when annealing temperatures are increased. Annealing of the mixtures also show positive effects for reducing mechanical losses and reducing optical absorption. This demonstrates their potential as an alternative high-index material for optical coatings in gravitational wave detectors with low-cost process.

1. Introduction

Gravitational-wave detectors (GWDs) such as Advanced LIGO (aLIGO), Advanced Virgo (AdvVirgo) and KAGRA are ground-based interferometric detectors utilizing high finesse optical cavities to perform high precision displacement measurements. The test mirrors of these GWDs consist of a high purity silica (SiO2) substrate coated with a high reflecting (HR) coating, Bragg's reflector alternating layers of low and high refractive-index amorphous materials typically deposited by ion-beam sputtering (IBS). LIGO and Virgo originally employed SiO2 and Ta2O5 as the low (n = 1.46) and high (n = 2.12) index materials, respectively. It is worth noting that for the mirror coating used by LIGO and Virgo, the major source of thermal noise was from Ta2O5, hindering the overall sensitivity of the GWD [1]. The low index material (i.e. SiO2) exhibited a minor contribution to this problem. To address this issue, aLIGO and AdvVirgo upgraded the mirror coatings to use TiO2:Ta2O5 mixture for the high index material [2], reducing mechanical losses (ϕ) by around 40% and increased the refractive index up to n = 2.19 [3]. This promising result led to new investigations and explorations for other oxide mixtures of high index that might feature low mechanical loss while preserving the high index or even augmenting it [4, 5, 6].

Investigations for various random network oxides showed that the annealed SiO2 and GeO2 mixed with Ta2O5 featured the lowest loss angles [4]. However, the Brownian thermal noise considers not only the loss angle of the material but also the total thickness of Bragg's reflector stack [7]. Investigative topic of interest is to achieve higher sensitivity by lowering mechanical losses in coatings, while maintaining required optical and thermal properties [8, 9]. Thus, ideal properties of the high index material comprise of low ϕ and high n at λ = 1064 nm. Unfortunately, it has been observed that a decrease in the mechanical loss leads to a decrease in the n of the

same material. For this reason, we investigated new deposition techniques as an alternative to IBS with aims to deposit low ϕ mixture materials while maintaining/increasing n.

This work presents a study of optical and mechanical properties of tantalum oxide and silicon oxide $(Ta_2O_5)_{1-x}(SiO_2)_x$ mixture coatings deposited by microwave plasma assisted co-sputtering technique with low optical absorption and low mechanical loss for gravitational wave detection. This deposition technique has advantages of being low cost and having high precise deposition control for stoichiometry of oxides, high deposition rate, low pinholes rate and good reproducibility [10, 11]. This paper also includes the investigations of the influence of thermal treatments on crystallinity, energy band change and mechanical loss of the mixtures.

2. Deposition Process and Characterization Methods

Deposition was carried out using a microwave plasma assisted pulsed DC reactive sputtering process. Within the deposition system there is a horizontal axis rotating drum in which deposition of each oxide layer can be achieved with multiple passes through rectangular planar DC magnetron sources and assisted microwave plasma oxidation region. The high deposition rate is obtained through the metal-like sputtering and a separated microwave plasma assisted oxidation reactive deposition which avoids target poisoning as the target surface has lower oxidation compared to standard sputtering [10, 12]. To produce the mixtures of Ta_2O_5 and SiO_2, two targets, Ta and Si, were mounted on left and right sides of chamber and sputtered simultaneously. The composition of mixtures was adjusted by varying the sputtering power of Ta target. Deposition system diagram can be found below in Figure 1. Detailed process parameters are shown in Table 1. Samples 1 and 2 are used to calibrate crystal monitoring. For mixtures, the deposition rate is the exactly the individual deposited layer thickness per rotation: because the drum rotates at 60 rpm, i.e. one revolution per second. Individual deposited layer thickness is in the range of Angstroms. Quartz crystals are used for thickness monitoring and calibrated for both targets separately prior to co-sputtering.

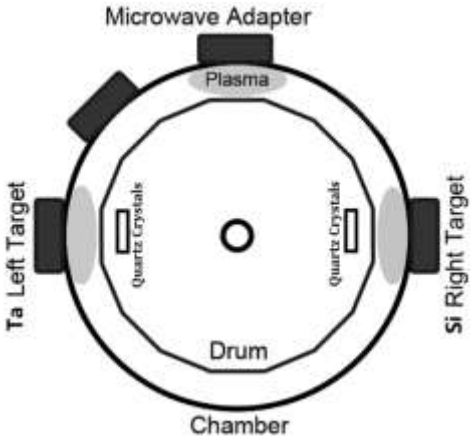

Fig 1. Schematic diagram of co-sputtering deposition system, with two simultaneously running targets to form mixtures and microwave plasma at the top to enhance oxidation, quartz crystals were used to monitor thickness

Table 1. Sample list and parameters of $(Ta_2O_5)_{1-x}$ $(SiO_2)_x$ mixed oxide films

No	Ta target, power control			Si target, voltage control			Expected Ta_2O_5 Volume Fraction
	P (KW)	D Rate (Å /s)	ET (nm)	V (V)	D Rate (Å /s)	ET (nm)	
1	3.5	2.7	500	0	0	0	1
2	0	0	0	400	0.85	500	0
3	3.5	2.7	380	400	0.85	120	0.76
4	2.4	1.9	345	400	0.85	155	0.69
5	1.5	1.1	256	400	0.85	244	0.51
6	0.9	0.6	207	400	0.85	293	0.41

Here P stands for sputtering power, V stands for sputtering voltage, D rate stands for deposition rate, ET stands for expected thickness.

For optical property analysis, samples were deposited on JGS3 substrates. For Ta_2O_5 samples, these can be directly deposited onto JGS3 substrate, as there is reasonable refractive index difference between Ta_2O_5 and JGS3 to produce necessary fringes for optical fitting. However, SiO_2 films have a similar refractive index to JGS3, thus an additional layer of Ta_2O_5 was deposited prior to SiO_2 deposition in order to have the necessary coherent fringes for optical fitting. n and k were obtained by fitting the transmission data obtained by a Perkin-Elmer Lambda 40 spectrometer and employing multiple Kim's oscillation model [13]. The data fitting was performed by using commercial software, SCOUT from W Theiss.

The Q factor measurements were performed by exciting a resonant mode of the sample and measuring the exponential decrease in the oscillation amplitude (ringdown) [14]. The coatings were deposited on pre-annealed (1000°C for 4 hours) fused silica substrates of diameter of 76.2 mm, thickness of 511±1μm and a flat of 25 mm, this is to remove residue stress and defects from substrates to prevent measurement errors. To test the gentle nodal suspension (GeNS), the cylindrical shaped sample is suspended on a silicon flat-convex lens with lens positioned over an aluminum platform and firmly held by a conical hole [14]. This GeNS was hosted inside a vacuum tank (<2×10^{-6} mbar), with He-Ne laser (λ = 633 nm and 4 mW) and a quadrant photodiode to measure the displacement of the sample excited at different resonant frequencies. Ringdown measurements recorded the decay of the excited resonant mode amplitude of the sample exhibiting damped harmonic motion, consisting of carrier and envelop signals, where the amplitude of the envelope can be represented by:

$$A(t) = A(0)\exp\left[-\pi f_0 \phi(f_0) t\right] \qquad (1)$$

The loss angle ϕ is defined as the ratio of the oscillation energy dissipation per cycle (P) to the elastic stored energy (E) [15] as below for substrate (ϕ_s) and coating (ϕ_c):

$$\phi_S = \frac{1}{\omega}\frac{P_S}{E_S} \qquad (2)$$

$$\phi_C = \frac{1}{\omega}\frac{P_C}{E_C} \qquad (3)$$

Where ω is the angular frequency. Experimentally, it is not possible to measure the mechanical loss of a coating (ϕ_c) alone. Experimentally, the mechanical losses of substrate and coated substrate can be obtained. The loss angle of coated substrate ϕ_{cs} can be expressed as:

$$\phi_{CS} = \frac{1}{\omega}\frac{P_S + P_C}{E_S + E_C} \quad (4)$$

Assuming Es ≫Ec as substrate is much thicker than coating layer, thus:

$$\phi_{CS} \approx \frac{1}{\omega}\frac{P_S + P_C}{E_S} = \frac{1}{\omega}\frac{\omega E_S \phi_S + \omega E_C \phi_C}{E_S} \quad (5)$$

By rearranging the above equation, at angular frequency ω_0, the mechanical loss of the coating can be calculated as follows:

$$\phi_C(\omega_0) = \frac{E_S}{E_C}\left[\phi_{CS}(\omega_0) - \phi_S(\omega_0)\right] \quad (6)$$

Where E_s/E_c is the ratio of the energy stored in substrate/coating, which were estimated by simulating using the finite element analysis method in software ANSYS package (Workbench 2021 Development R2) [16] based on mechanical properties (such as Young's Modulus, Poisson's Ratio) of substrate and coating as well as the measured data of wafer vibrations.

For microstructure analysis, X-ray Diffraction (XRD) were done using SIMENS D5000. After this, all the mixture samples were annealed at the various temperatures, the above analyses were then iterated to investigate the changes.

3. Optical Properties of the Co-sputtered Films of Tantalum Oxide and Silicon Oxide as Deposited

Figure 2 shows the n and k represented as a function of wavelength (λ). The extinction coefficient is not accurate enough for low absorption material due to the transmittance measurement accuracy of spectrophotometer, however the refractive index obtained has good accuracy, particularly at the wavelength of 1064 nm, for Ta_2O_5 and SiO_2. From Figure 2, one could conclude that for near UV regions, n of the resulting mixture decreases with Ta_2O_5 volume fraction, and the absorption of mixture decreases when Ta_2O_5 is mixed with SiO_2, particularly for the 300 nm absorption edge of Ta_2O_5/SiO_2 mixture (see Figure 2 insert).

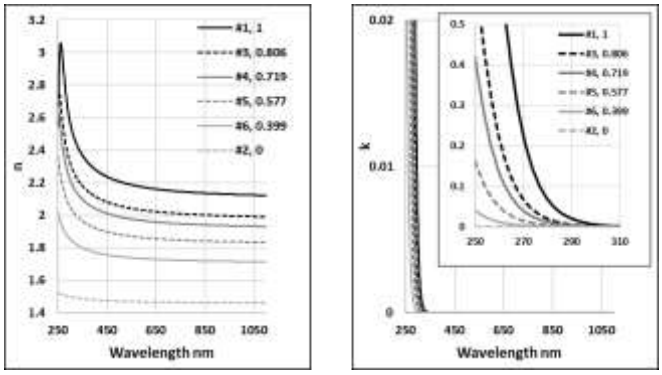

Figure 2. Wavelength dependence of the n and k for $(Ta_2O_5)_{1-x}(SiO_2)_x$ co-sputtered coatings as deposited. The legend shows sample number and the measured Ta_2O_5 fraction

Based on optical properties of the mixture, the volume ratio can be obtained by using a generalized anisotropic Bruggeman Effective Medium Approximation (EMA) [17]. The actual coatings consist of the stacks of alternative layers of tantalum oxide and silicon oxide with thickness in the angstrom range. As there are only two phases in our samples, this EMA equation can be simplified to:

$$f_1\frac{\varepsilon_1 - \varepsilon}{\varepsilon_1 + 2\varepsilon} + (1 - f_1)\frac{\varepsilon_2 - \varepsilon}{\varepsilon_2 + 2\varepsilon} = 0 \quad (7)$$

Where the dielectric constants for phase 1 (Ta_2O_5, ε_1), phase 2 (SiO_2, ε_2) and the mixture (ε) are known. Volume fraction of Ta_2O_5 (f_1) can then be calculated using Eq (7) with the results shown in Table 2.

Table 2. Calculated volume fraction of Ta_2O_5 and refractive index at λ = 1064 nm

No	*n*	ε	EVF of Ta_2O_5	CVF of Ta_2O_5	ET (nm)	FT (nm)
1	2.122	4.503	1	1	500	486.9
2	1.460	2.132	0	0	500	533.0
3	1.990	3.960	0.76	0.806	500	492.4
4	1.930	3.725	0.69	0.719	500	487.8
5	1.833	3.360	0.51	0.577	500	467.7
6	1.713	2.934	0.41	0.399	500	502.0

Here EVF stands for Expected Volume Fractions, CVF stands for Calculated Volume Fractions, ET stands for Expected Thickness, FT stands for Fitted Thickness

Discrepancy between calculated and expected volume fractions may be from in-situ deposition rate reading accuracy as the reading for deposition rate on IC5 (INFICON IC/5 Thin Film Deposition Controller) is angstrom level and only has 2 digits. It should be noted that only samples 1 and 2 (pure Ta_2O_5 and pure SiO_2) are calibrated, this calibration was then used to plan mixture samples 3 to 6 with estimated expected volume fractions. The deposition of samples 3 to 6 were monitored in-situ.

4. Mechanical Loss of the Co-sputtered films of Tantalum Oxide and Silicon Oxide as Deposited

The resulting mechanical loss angles, ϕ_s, ϕ_c and ϕ_{cs} for all materials are summarized in Table 3. The table also includes the substrate/coating energy ratio (E_s/E_c) for the first fundamental resonant mode extracted using ANSYS and for calculating ϕ_c by using Eq 6.

Table 3. Mechanical Loss Angles of Single Layer Coatings Measured at First Resonant Mode

No	Ta_2O_5 CVF	F (Hz)	ϕ_s ($\times 10^{-6}$)	ϕ_{cs} ($\times 10^{-6}$)	E_s/E_c	ϕ_c ($\times 10^{-4}$)
1	1.000	530.62	1.82 ± 0.01	12±2	148.04	14±4
3	0.806	527.95	4.11 ± 0.06	10.9±0.4	147.71	10.3±0.5
4	0.719	532.96	1.71 ± 0.01	5.2±0.5	148.74	5.7±0.7
5	0.577	528.53	1.35 ± 0.01	5.1±0.4	147.46	5.9±0.6
6	0.399	532.61	2.52 ± 0.01	6.2±0.6	148.56	5.7±0.9
2	0.000	521.43	3.83 ± 0.02	9.6±0.6	246.14	15±2

Here CVF stands for Calculated Volume Fractions for Ta_2O_5, F for frequency of first resonance mode

Results show that coating loss of mixed oxide films are in the range of 10^{-3} to 10^{-4}, where Ta_2O_5 volume fraction of 39.9% (i.e., SiO_2 volume fraction is 60.1%) results in a much-reduced mechanical loss angle: $5.7\pm0.9 \times 10^{-4}$ without annealing treatment. These results are promising since the application of thermal annealing is expected

to further reduce mechanical loss of coatings. The purpose of the investigation is to develop an alternative for high-index materials for reflector and our results (currently without annealing and were deposited by magnetron sputtering) is of comparable order to previously reported annealed samples deposited via Ion Beam Sputtering. For example, Ta2O5 and SiO2 mixtures range between 2 to 5 x 10^{-4}, while TiO_2 and Ta_2O_5 mixtures range between 2 and 3 x 10^{-4} [1, 3].

5. The Influence of Annealing Treatment on the Mixtures

Our magnetron sputtering deposited Ta_2O_5/SiO_2 mixtures were annealed at the following temperatures: 200, 400, 600 and 700°C for a duration of 2 hours. XRD results show that the mixture coatings were changed from amorphous to polycrystalline after annealing at 700°C for the pure Ta_2O_5 sample, as shown in Figure 3a. For the samples #2 to #6, pure SiO_2 and mixture samples, XRD spectrum does not show the phase transition, see examples given in Figure 3b.

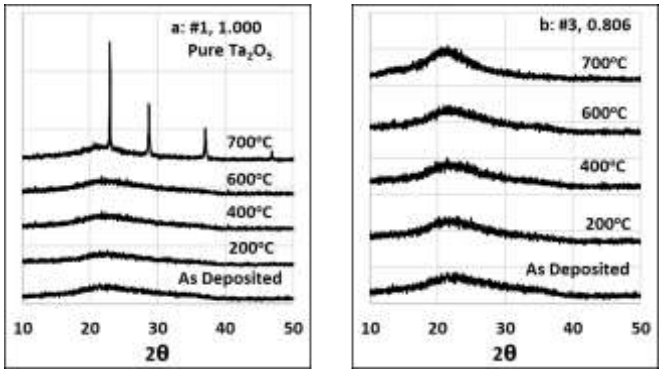

Fig.3 a) XRD spectra of pure annealed Ta_2O_5, b) example XRD spectra for Ta_2O_5/SiO_2 mixture coatings with CVF of Ta_2O_5 = 0.806

5.1. Optical Properties of Annealed Mixture Coatings

O'Leary-Johnson-Lim (OJL) Model [18] was used to extract information such as energy band structure and crystallinity. In order to give better explanation for the physical meaning of the changes in optical properties following annealing process, the equations of the density of states (DOS) functions are shown below. In the equations, the energy band gap can be expressed as $E_{g0} = V_c - V_v$, where V_v and V_c are ground state energies for the valence and conduction bands respectively. γ is the disorder constant which represents the breadth of the band tails (Urbach tails) [19, 20, 21, 22]. This means that the higher γ-value corresponds to higher degrees of the amorphous state. As an extreme example, for a perfect crystal, the disorder constant γ→0. Following from this, equations 8 to 10 can be obtained to express a perfect crystal and its DOS follows a parabolic shape.

In the equations, m_c^* represents a DOS effective mass which we associate with the conduction band, h represents the Planck constant and $N_c(E)$ is the density of state at energy E. We assume that the conduction band DOS function is:

$$N_c(E) = \frac{8\sqrt{2}\cdot\left(m_c^*\right)^{3/2}\pi}{h^3}\begin{cases}\sqrt{E-V_c}, & E \geq V_c + \dfrac{\gamma_c}{2} \\ \sqrt{\dfrac{\gamma_c}{2}}\exp\left(-\dfrac{1}{2}\right)\exp\left(\dfrac{E-V_c}{\gamma_c}\right), & \\ E < V_c + \dfrac{\gamma_c}{2} & \end{cases} \quad (8)$$

Similarly, we assume that the valence band DOS function is:

$$N_v(E) = \frac{8\sqrt{2}\cdot\left(m_v^*\right)^{3/2}\pi}{h^3}\begin{cases}\sqrt{V_v-E}, & E < V_v - \dfrac{\gamma_v}{2} \\ \sqrt{\dfrac{\gamma_v}{2}}\exp\left(-\dfrac{1}{2}\right)\exp\left(\dfrac{V_v-E}{\gamma_v}\right), & \\ E \geq V_v - \dfrac{\gamma_v}{2} & \end{cases} \quad (9)$$

And for perfect crystals where γ→0:

$$N_c(E) = \frac{8\sqrt{2}\cdot\left(m_v^*\right)^{3/2}\pi}{h^3}\begin{cases}\sqrt{E-V_c}, & E \geq V_c \\ 0, & E < V_c\end{cases} \quad (10)$$

Using the above equations and the OJL model, the transmittance of all annealed mixture coatings was fitted and the obtained energy band gap and disorder constants γ were extracted by data fitting, as shown in Table 4. Figure 4 is an example plot to demonstrate the transmittance fitting. Figure 5 is the calculated extinction coefficients from fitting and demonstrate the trend of reducing extinction coefficients with increasing annealing temperature.

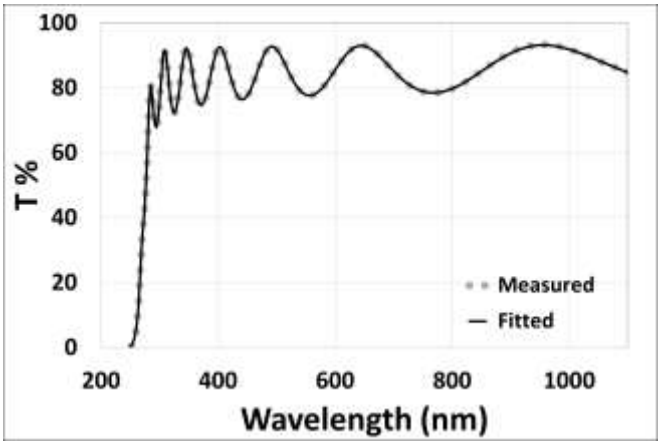

Fig.4 An example of the measured and fitted transmittance of sample #4 annealed at 600°C for 2 hours

Table 4. Energy Band Gap and Disorder Constant Obtained by Transmittance Fitting of Mixture Coatings with Various Annealing Temperatures

No	Ta2O5 CVF	eV	As deposited	200°C	400°C	600°C
1	1.000	E_{g0}	4.235	4.246	4.270	4.273
		γ	0.0777	0.0767	0.0743	0.0740
2	0.000	E_{g0}	-	-	-	-
		γ	-	-	-	-
3	0.806	E_{g0}	4.380	4.391	4.404	4.399
		γ	0.0854	0.0862	0.0797	0.0789
4	0.719	E_{g0}	4.438	4.454	4.466	4.459
		γ	0.0850	0.0882	0.0814	0.0809
5	0.577	E_{g0}	4.547	4.562	4.570	4.555
		γ	0.0867	0.0892	0.0834	0.0842
6	0.399	E_{g0}	4.674	4.691	4.696	4.675
		γ	0.0905	0.0942	0.0876	0.0880

Here CVF stands for Calculated Volume Fractions for Ta_2O_5, Pure SiO2 bandgap was found via extrapolation at 8.204 eV, which is very close to reported value 8.8 to 8.9 eV [23], however this is beyond our measurement range thus the results are not included in the table

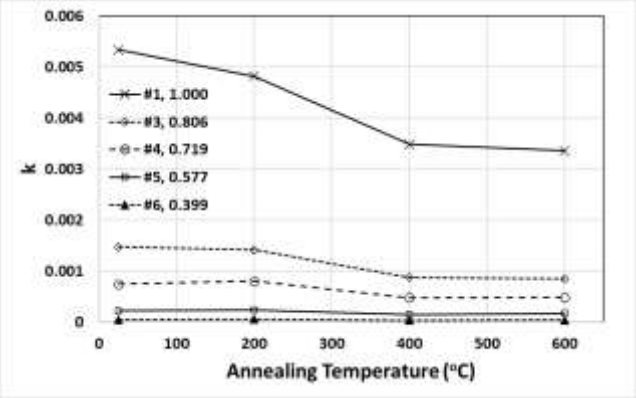

Fig. 5 Fitted extinction coefficients of mixture samples at 300nm and various annealing temperature

As shown in the table, energy band gap increases as SiO_2 concentration increases and disorder constant decreases with the increase to annealing temperatures. This means the degree of crystallinity of the coatings are increased with increase of temperature as per indicated by the physical meaning of disorder constant. This also indicates that the defects in coatings are reduced by annealing. This will further contribute to the reduction in the mechanical loss of the mixture coatings. However, sample #2 is SiO2, the absorption edge is around 140 nm which is not in the range of our spectrometer, therefore the energy band gap and disorder constants for this sample were extrapolated and not included in the table.

5.2. Mechanical Loss of Annealed Mixture Coatings

The mechanical losses of the annealed samples were analyzed using same method as described in section 4. To simplify the discussion, only the mechanical losses of coatings are presented in Figure 6. The results indicate that all annealed samples have reduced mechanical loss when compared to the samples pre-annealing treatment, for all frequencies. It should be noted that the reduction of mechanical loss with annealing is more significant at higher frequencies. For example, the mechanical loss of Ta_2O_5 with 80.6% volume fraction (sample #3) was reduced from 1.0 x 10^{-3} for as deposited sample to 4.0 x 10^{-4} for the sample annealed at 400°C and measured at 528 Hz, particularly note reduction of mechanical loss down to 1.0 x 10^{-4} at 6790 Hz. The figure 5 also confirmed that the mechanical loss angle decreases with the annealing temperature for all the mixture samples analyzed at various frequencies, particularly mechanical loss is down to 3.0 x 10^{-5} for sample #4 at 6790 Hz (circled). This would be very promising for applications in GWD.

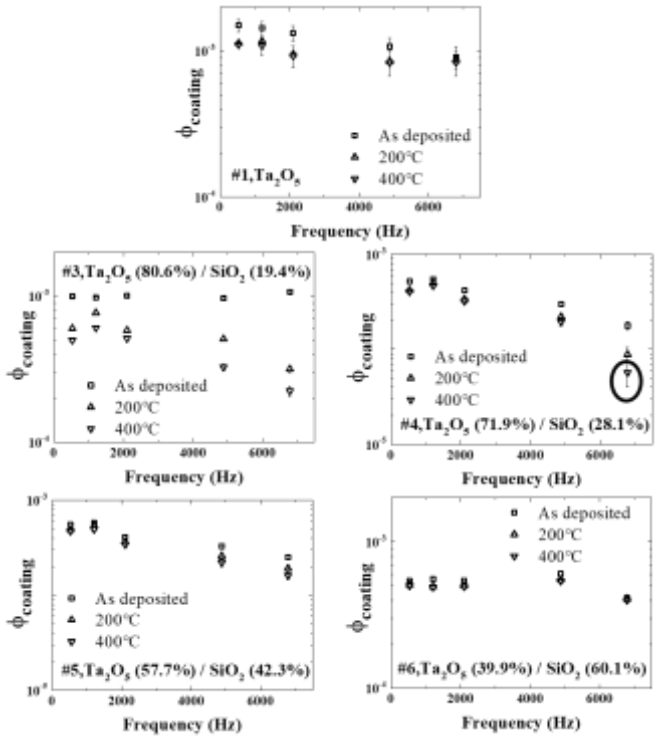

Fig 6, Mechanical loss measurement results for Ta_2O_5/SiO_2 mixture coatings after annealing. Circle indicates point of interest where the mechanical loss was reduced to 3 x 10^{-5} at 6790 Hz

6. Conclusions

In this work, we demonstrate an alternative deposition technique to IBS to achieve deposition of low mechanical loss materials (3 x 10^{-5}) with high refractive index (1.93) while maintaining low processing costs (sample #4). It can become a candidate for high index material alternative for GWD reflectors. Our deposition process using microwave plasma enhanced co-sputtering for tantalum oxide and silicon oxide mixture coatings offer advantages with high precision deposition control for oxide stoichiometry, high deposition rate, good reproducibility and low costs. Annealing of the mixtures also show positive effects for reducing mechanical losses and reducing optical absorption. XRD results show that the Ta_2O_5 sample has clear phase transition from amorphous to polycrystalline when annealed at 700°C for 2 hours. This phase change is not seen for the other samples. Transmittance fitting show that energy band gap increases as SiO2 concentration increases and disorder constant decreases when annealing temperatures are increased. Mechanical loss measurements show that all annealed samples have reduced mechanical loss compared to the as deposited samples, with this reduction trend being more significant for lower measurement frequencies. Optical analysis and

mechanical measurements are in agreement in microstructure change (disorder constants) brought on by annealing treatment. Combining the conclusions of optical and mechanical results, the microwave plasma assisted co-sputtering is a possible low-cost process to produce promising alternative high-index materials for GWD applications. Further investigations are planned for detailed exploration of this potential, including improved absorption measurements at wavelengths of interest (1064, 1550 and 2000 nm) using photo-thermal common-path interferometry for low optical absorption.

Acknowledgments. Authors would like to thank the University of the West of Scotland, University of Strathclyde, University of Glasgow, and Science and Technology Facilities Council (STFC) for financial support (ST/V005626/1). Authors also thank their colleagues within LIGO Scientific Collaboration for advice & support

Disclosures. The authors declare no conflicts of interest.

Data availability. Data underlying the results presented in this paper are not publicly available at this time but may be obtained from the authors upon reasonable request.

References

1. S. D. Penn, P. H. Sneddon, H. Armandula, J. C. Bet- zwieser, G. Cagnoli, J. Camp, D. Crooks, M. M. Fejer, A. M. Gretarsson, G. M. Harry, J. Hough, S. E. Kittelberger, M. J. Mortonson, R. Route, S. Rowan and C. C. Vassiliou, "Mechanical loss in tantala/silica dielectric mirror coatings", Classical and Quantum Gravity **20**, 2917 (2003).
2. M. Granata, A. Amato, L. Balzarini, M. Canepa, J. De- gallaix, D. Forest, V. Dolique, L. Mereni, C. Michel, L. Pinard, B. Sassolas, J. Teillon and G. Cagnoli, "Amorphous optical coatings of present gravitational-wave interferometers", Classical and Quan- tum Gravity **37**, 095004 (2020).
3. M. Granata, E. Saracco, N. Morgado, A. Cajgfinger, G. Cagnoli, J. Degallaix, V. Dolique, D. Forest, J. Franc, C. Michel, L. Pinard and R. Flaminio, "Mechanical loss in state-of-the-art amorphous optical coatings", Physical Review D **93**, 012007 (2016).
4. M. A. Fazio, G. Vajente, L. Yang, A. Ananyeva and C. S. Menoni, "Comprehensive study of amorphous metal oxide and Ta2O5-based mixed oxide coatings for gravitational-wave detectors", Phys. Rev. D **105**, 102008 (2022)
5. G. Vajente, L. Yang, A. Davenport, M. Fazio, A. Ananyeva, L. Zhang, G. Billingsley, K. Prasai, A. Markosyan, R. Bassiri, M. M. Fejer, M. Chicoine, F. Schiettekatte and C. S. Menoni, "Low Mechanical Loss TiO2:GeO2 Coatings for Reduced Thermal Noise in Gravitational Wave Interferometers", Phys. Rev.Lett. **127**, 071101 (2021)
6. M. Abernathy, A. Amato, A. Ananyeva, et al, "Exploration of co-sputtered Ta2O5–ZrO2 thin films for gravitational-wave detectors", Classical and Quantum Gravity **38**, 195021 (2021)
7. A. Amato, G. Cagnoli, M. Granata, B. Sassolas, J. Degallaix, D. Forest, C. Michel, L. Pinard, N. Demos, S. Gras, M. Evans, A. Di Michele and M. Canepa, "Optical and mechanical properties of ion-beam sputtered Nb2O5 and TiO2−Nb2O5 thin films for gravitational-wave interferometers and an improved measurement of coating thermal noise in Advanced LIGO", Phys. Rev. D **103**, 072001 (2021)
8. V. B. Braginsky, M. L. Gorodetsky and S. P. Vyatchanin, "Compendium of thermal noises in optical mirrors", in *Optical Coatings and Thermal Noise in Precision Measurement* G. Harry, T. P.Bodiya and R. DeSalvo, eds. (Cambridge University Press, 2012)
9. G. M. Harry, H. Armandula, E. Black, D. R. M. Crooks, G. Cagnoli, J. Hough, P. Murray, S. Reid, S. Rowan, P. Sneddon, M. M. Fejer, R. Route and S. D. Pen, "Thermal noise from optical coatings in gravitational wave detectors", Appl. Opt. **45**, 1569-1574 (2006)
10. S. Song, C. Li, H. Chu and D. Gibson, "Reactive dynamics analysis of critical Nb2O5 sputtering rate for drum-based metal-like deposition", Applied Optics **56**, C206 (2017)
11. L. Hang, W. Liu, S. Song, D. Gibson, S. Zhou, X. Zhang, C. Li and S. Ahmadzadeh, Simulation analysis and preparation of a high optical density laser protection filter, Applied Optics **59**, 3315 (2020)
12. C. Li, S. Song, D. Gibson, D. Child, H. Chu and E. Waddell, "Modeling and validation of uniform large-area optical coating deposition on a rotating drum using microwave plasma reactive sputtering", Applied Optics **56**, 65 (2017)
13. C. C. Kim, J. W. Garland, H. Abad and P. M. Raccah, "Modeling the optical dielectric function of semiconductors: Extension of the critical-point parabolic-band approximation", Phys. Rev. B **45**, 11749 (1992)
14. E. Cesarini, M. Lorenzini, E. Campagna, F. Martelli, F. Piergiovanni, F. Vetrano, G. Losurdo and G. Cagnoli, "A "gentle" nodal suspension for measurements of the acoustic attenuation in materials", Review of Scientific Instruments **80**, 053904 (2009)
15. L. Kuo, H. Pan, S. Huang and S. Chao, "Mechanical Loss Angle Measurement for Stressed thin Film Using Cantilever Ring-Down Method", Materials Research **21**, e20170869 (2018)
16. ANSYS Inc and ANSYS Europe Ltd, "ANSYS Workbench Products Release Notes", August 2005
17. M. Foldyna, R. Ossikovski, A. D. Martino, B. Drevillon, K. Postava, D. Ciprian, J. Pištora and K. Watanabe, "Effective medium approximation of anisotropic lamellar nanogratings based on Fourier factorization", Optics Express **14**, 3114-3128 (2006).
18. S. K. O'Leary, S. R. Johnson and P. K. Lim, "The relationship between the distribution of electronic states and the optical absorption spectrum of an amorphous semiconductor: An empirical analysis", Journal of Applied Physics **82**, 3334-3340 (1997)
19. A. Amato, S. Terreni, M. Granata, C. Michel, B. Sassolas, L. Pinard, M. Canepa and G. Cagnoli, "Observation of a Correlation Between Internal friction and Urbach Energy in Amorphous Oxides Thin Films", Scientific Reports **10**, 1670 (2020)
20. D. A. Drabold, Y. Li, B. Cai and M. Zhang, "Urbach tails of amorphous silicon", Phys. Rev. B **83**, 045201 (2011)
21. D. A. Drabold, "Topics in the theory of amorphous materials", The European Physical Journal B **68**, 1–21 (2009)
22. H. Chu, Q. Wand, Y. Shi, S. Song, W. Liu, S. Zhou, D. Gibson, Y. Alajlani and C. Li, "Structural, optical properties and optical modelling of hydrothermal chemical growth derived ZnO nanowires", Trans. Nonferrous Met. Soc. China **30**, 191−199 (2020)
23. D. A. Tashmukhamedova and M. B. Yusupjanova, "Emission and optical properties of SiO2/Si thin films", J. Surf. Inv. X-ray, Synchrotron and Neutron Tech **10**, 1273–1275 (2016)